



Cite this: *RSC Adv.*, 2025, **15**, 20125

A mercury complex-based fluorescent sensor for biological thiols[†]

Nguyen Khoa Hien, ^a Trinh Thi Giao Chau, ^a Nguyen Dinh Luyen, ^b Quan V. Vo, ^c Mai Van Bay, ^d Son Tung Ngo, ^{ef} Pham Cam Nam ^{*g} and Duong Tuan Quang ^{*b}

A novel fluorescent sensor, $\text{Hg}(\text{DST})_2$, was developed for the selective detection of biological thiols, including glutathione (GSH), cysteine (Cys), and homocysteine (Hcy), in fully aqueous solutions at pH 7.2. The sensor exhibited significant fluorescence quenching upon coordination with Hg^{2+} , which was reversibly restored in the presence of thiols due to the formation of thermodynamically favored Hg -thiol complexes. The OFF-ON fluorescence mechanism of the sensor was elucidated using DFT calculations. Fluorescence titration experiments revealed a strong linear correlation ($R^2 \approx 0.998$) between fluorescence intensity and thiol concentrations within the ranges of 0.34–8.00 μM for GSH, 0.47–10.00 μM for Cys, and 0.26–8.00 μM for Hcy, with corresponding limits of detection (LOD) of 0.34, 0.47, and 0.26 μM , respectively. The sensor demonstrated high selectivity toward thiols in the presence of common amino acids, metal ions, and anions, with interference from Ag^+ , Cu^{2+} , Co^{2+} , and Ni^{2+} mitigated using 1,10-phenanthroline (PHEN). Owing to its high sensitivity, selectivity, and water solubility, $\text{Hg}(\text{DST})_2$ represents a promising tool for thiol quantification in biological and environmental matrices.

Received 1st April 2025
Accepted 5th June 2025

DOI: 10.1039/d5ra02268a
rsc.li/rsc-advances

1. Introduction

Cysteine (Cys), glutathione (GSH), and homocysteine (Hcy) are non-protein biological thiols that play crucial roles in various physiological and biochemical functions in humans.^{1–3} In particular, Cys is a precursor for protein synthesis and plays a vital role in protecting cells from damage caused by free radicals and oxidative agents. Additionally, Cys is involved in detoxification processes by binding to heavy metals and other toxic substances, aiding in their removal from the body.⁴ The intracellular concentration of Cys ranges from 30 to 200 μM .⁵ The highest concentration of Cys in plasma has been found to reach up to 250 μM .¹ Changes in Cys levels have been shown to be associated with several diseases such as Alzheimer's and

Parkinson's disease, autoimmune deficiency syndrome, and hyperhomocysteinemia.¹

Glutathione is a tripeptide made up of three amino acids: L-glutamate, L-cysteine, and L-glycine. It is the most abundant non-protein thiol in cells, with intracellular concentrations ranging from 1 to 15 mM, primarily in its reduced form.⁶ GSH is one of the body's most powerful antioxidants, protecting cells from oxidative damage by neutralizing free radicals.^{6,7} It plays a critical role in detoxification, particularly in the liver, where it helps eliminate harmful substances and convert them into less toxic forms.⁸ Additionally, GSH is essential for maintaining and regulating the immune system.⁶ It is also believed to be associated with diseases, including cancer, stroke, heart disease, pancreatic and kidney disorders, diabetes, Alzheimer's, Parkinson's, gastritis, peptic ulcers, and atherosclerosis diseases.^{6,7}

Homocysteine (Hcy) is a metabolic intermediate formed during the catabolism of methionine in the one-carbon metabolism cycle. It participates in methylation processes, methionine regeneration, and cysteine biosynthesis, with its homeostasis maintained through pathways that either regenerate methionine or convert it to cysteine.⁹ Typical blood Hcy levels range from 5 to 13 μM .¹⁰ Elevated Hcy levels, a condition known as hyperhomocysteinemia, are linked to cardiovascular, neurological, and bone-related disorders, as well as fertility issues, including recurrent miscarriages and infertility in both genders.^{11–14}

Given the important roles of Cys, GSH, and Hcy, various methods for their determination have been developed, including high-performance liquid chromatography,^{1,15} gas

^aMientrung Institute for Scientific Research, Vietnam National Museum of Nature, Vietnam Academy of Science and Technology, Hue 49000, Vietnam

^bDepartment of Chemistry, Hue University, Hue 49000, Vietnam. E-mail: duongtuanquang@dhspue.edu.vn

^cFaculty of Chemical Technology-Environment, The University of Danang - University of Technology and Education, 48 Cao Thang, Danang 50000, Vietnam

^dThe University of Danang, University of Science and Education, Danang 50000, Vietnam

^eLaboratory of Biophysics, Institute for Advanced Study in Technology, Ton Duc Thang University, Ho Chi Minh City 72915, Vietnam

^fFaculty of Pharmacy, Ton Duc Thang University, Ho Chi Minh City 72915, Vietnam

^gThe University of Danang, University of Science and Technology, Danang 50000, Vietnam. E-mail: pcnam@ dut.udn.vn

† Electronic supplementary information (ESI) available. See DOI: <https://doi.org/10.1039/d5ra02268a>



chromatography-mass spectrometry,¹⁶ electrochemistry,¹⁷ and UV-Vis absorption and fluorescence spectroscopy.^{18–20} Among these, fluorescent sensors have garnered significant interest from scientists due to their high sensitivity, simple analysis methods, and ability to monitor in living cells.^{21–24}

Some recently reported fluorescent sensors for biothiol detection based on metal ion complexes are summarized in Table 1. Most reported fluorescent sensors do not selectively detect individual biothiols because Cys, GSH, and Hcy have similar structures.²⁵ Nevertheless, this limitation does not diminish the efforts to develop new fluorescent sensors for biothiols. This is because, in practice, there are cases where only the concentration change of a specific biothiol related to a particular disease is of interest, such as monitoring glutathione levels in the liver to assess liver function or monitoring homocysteine levels in the blood to evaluate the risk of cardiovascular diseases and stroke.^{26–28} Additionally, different biothiols are distributed differently in various body parts. For example, the concentrations of cysteine and glutathione are highest in tissues, particularly in the liver, while homocysteine is usually undetectable in tissues and is primarily found in plasma.^{29–31} Notably, fluorescent sensors often interact reversibly with biothiols, which is very useful for monitoring real-time changes in biothiol concentrations, and providing detailed information about pathological conditions.¹⁰

In this study, we report a fluorescent sensor ($\text{Hg}(\text{DST})_2$) that can detect the real-time concentrations of Cys, GSH, and Hcy, based on the complex of a fluorescent compound **DST** with Hg^{2+} ions. The $\text{Hg}(\text{DST})_2$ complex interacts reversibly with Cys, GSH, and Hcy, releasing **DST**, accompanied by a fluorescence signal change from *OFF* to *ON* at 445 nm. This process can be reversed at least five times by alternating the addition of Hg^{2+} and biothiols.

and Hcy, releasing **DST**, accompanied by a fluorescence signal change from *OFF* to *ON* at 445 nm. This process can be reversed at least five times by alternating the addition of Hg^{2+} and biothiols.

2. Materials and methods

2.1. Instruments

The structural characteristics of the compounds were determined through the study of ^1H NMR, ^{13}C NMR, and mass spectra, using a Bruker Ascend 600 spectrometer for NMR and an Agilent 6200 series TOF LC/MS system for mass spectrometry. The absorption and fluorescence properties of the compounds were studied using Shimadzu spectrometers, with the UV-1800 for UV-Vis absorption spectra and the RF-5301 PC Series for fluorescence spectra.

2.2. Reagents

All chemicals used were purchased from Merck. Among them, 4-(diethylamino)salicylaldehyde and aminothiourea were of synthesis grade. The solvents used were of HPLC grade. The metal salts, amino acids, and biothiols (Cys, GSH, and Hcy) were of analytical purity grade.

2.3. Computational methodology

Density Functional Theory (DFT) calculations were performed using the Gaussian 16 software at the PBE0/LanL2dz level of theory.^{41–45} Time-Dependent Density Functional Theory (TD-DFT) method was employed to investigate the excited

Table 1 Some fluorescent sensors for biothiol detection based on metal ion complexes

Complexes of metal ions	Detectable biothiols	LOD (μM)	Solvent/pH	The influence of other thiols	Ref.
Cu^{2+}	GSH	0.16	HEPES/DMSO (95/5, v/v), pH 7.4	Affected by Cys and Hcy	32
Cu^{2+}	GSH	0.80	DMF/HEPES (3/7, v/v), pH 7.4	Cannot detect individual thiols separately	33
	Cys	1.00			
	Hcy	1.50			
Cu^{2+}	GSH	0.30	Ethanol/HEPES (1/1, v/v), pH 7.4	Cannot detect individual thiols separately	19
	Cys				
	Hcy				
Cu^{2+}	Cys	0.17	$\text{CH}_3\text{CN}/\text{HEPES}$ (1/1, v/v), pH 7.4	- Cannot detect individual thiols separately	34
	Hcy	0.25		- The influence of GSH has not been reported	
Cu^{2+}	GSH	0.20	$\text{CH}_3\text{OH}/\text{HEPES}$ (9/1, v/v), pH 7.2	The influence of Cys and Hcy has not been reported	35
Cu^{2+}	GSH	0.44	DMF/HEPES (7:3, v/v), pH 7.4	Cannot detect individual thiols separately	36
	Cys	0.96			
	Hcy	0.68			
Cu^{2+}	Cys	0.015	$\text{CH}_3\text{CN}/\text{HEPES}$ (7/3, v/v), pH 7.4	The influence of GSH and Hcy has not been reported	37
Hg^{2+}	Cys	0.20	Ethanol/HEPES (1:9, v/v), pH 7.4	Affected by GSH and Hcy	20
Hg^{2+}	Cys	0.016	CH_3CN	The influence of GSH and Hcy has not been reported	38
Ag^+	GSH	0.208	Dioxane/Tris- HClO_4 (3/7, v/v), pH 7.4	Cannot detect individual thiols separately	39
	Cys	0.089			
	Hcy	0.174			
Fe^{3+}	Cys	0.45	Water (1% DMSO) pH: 2–11	Not affected by GSH and Hcy	40



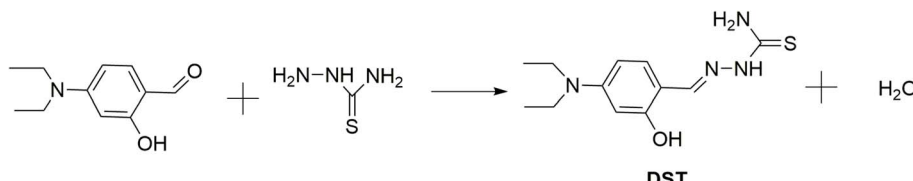


Fig. 1 The reaction scheme for the synthesis of the DST fluorescent compound.

states.^{45,46} Solvent calculations were carried out using the Polarizable Continuum Model (PCM).⁴⁷

3. Results and Discussion

3.1. Synthesis and characterization of the $\text{Hg}(\text{DST})_2$ sensor

The **DST** fluorescent compound was synthesized according to the reaction shown in Fig. 1, as previously reported.⁴⁸ Briefly, equimolar solutions of aminothiourea and 4-(diethylamino) salicylaldehyde were refluxed in ethanol with anhydrous sodium sulfate at 85 °C under a nitrogen atmosphere for 8 hours, followed by stirring at ambient temperature for 12 hours. The reaction mixture was filtered to remove sodium sulfate, purified *via* silica gel column chromatography using a chloroform : methanol (70 : 1, v/v) eluent, and the solvent was evaporated under reduced pressure, yielding **DST** with an approximate efficiency of 71.4% (^{13}C NMR, ^1H NMR, and MS spectra are provided in Fig. S1–S3 of the ESI data[†]).

Experimental results in Fig. 2 showed that **DST** exhibited a fluorescence spectrum with a maximum wavelength at 445 nm, with an excitation wavelength at 368 nm. **DST** reacted with Hg^{2+} in a 2 : 1 molar ratio, accompanied by approximately 95% fluorescence quenching. The Stern–Volmer plot for the fluorescence quenching of **DST** by Hg^{2+} (Fig. S4[†]) showed that the relationship between the ratio F_0/F and the concentration Q of Hg^{2+} (where F_0 and F were the fluorescence intensities of the **DST** solution in the absence and presence of Hg^{2+} at concentration Q , respectively) was not linear but exhibited an upward (positive) deviation. This suggested that both static and dynamic quenching mechanisms were responsible for the observed decrease in fluorescence intensity.^{49,50}

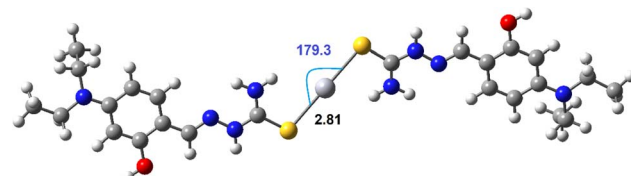


Fig. 3 The stable structure of $\text{Hg}(\text{DST})_2$ sensor at the DFT/PBEO/Lanl2dz.

The stable structure of the complex between **DST** and Hg^{2+} in a 2 : 1 molar ratio was determined at the DFT/PBEO/Lanl2dz and is presented in Fig. 3. The calculation results show that the $\text{Hg}(\text{DST})_2$ complex is stabilized by two $\text{Hg}\cdots\text{S}$ interactions, with a contact distance of 2.81 Å, which is significantly smaller than the van der Waals radius sum of Hg and S atoms, which is 3.35 Å. The $\text{Hg}\cdots\text{S}\cdots\text{Hg}$ bond angle is nearly linear, with a value of 179.3°.⁵¹ The two **DST** molecules in the complex are not in the same plane but lie in two parallel planes (considering only the π -conjugated system plane).

The results of the study on the singlet electron transition process from the ground state S_0 to the excited state S_1 (Fig. 4) indicated that in the **DST** compound, this process was determined by the electron transition from HOMO to LUMO (oscillator strength $f = 1.2441$). Meanwhile, in the $\text{Hg}(\text{DST})_2$ complex, this process was determined by the electron transition from HOMO – 1 to LUMO ($f = 0.5515$). Therefore, in the excited state, the $\text{Hg}(\text{DST})_2$ complex underwent a photoinduced electron transfer (PET) process with the transfer of an electron from HOMO to HOMO – 1, leading to the absence of an excited electron transition from LUMO to HOMO – 1 (which would

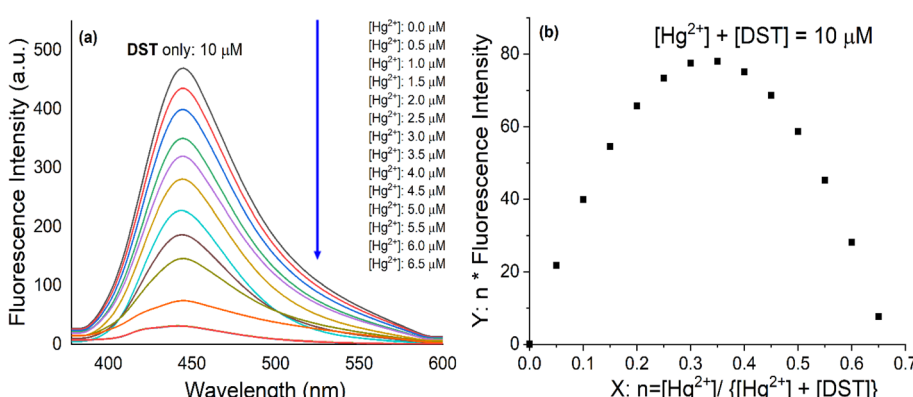


Fig. 2 (a) The fluorescence titration spectra of DST solution (10 μM) with Hg^{2+} at concentrations ranging from 0 to 6.5 μM ; (b) Job's plot of the interaction between Hg^{2+} and DST (in pH 7.2 phosphate buffer, with an excitation wavelength of 368 nm, an emission wavelength of 445 nm).



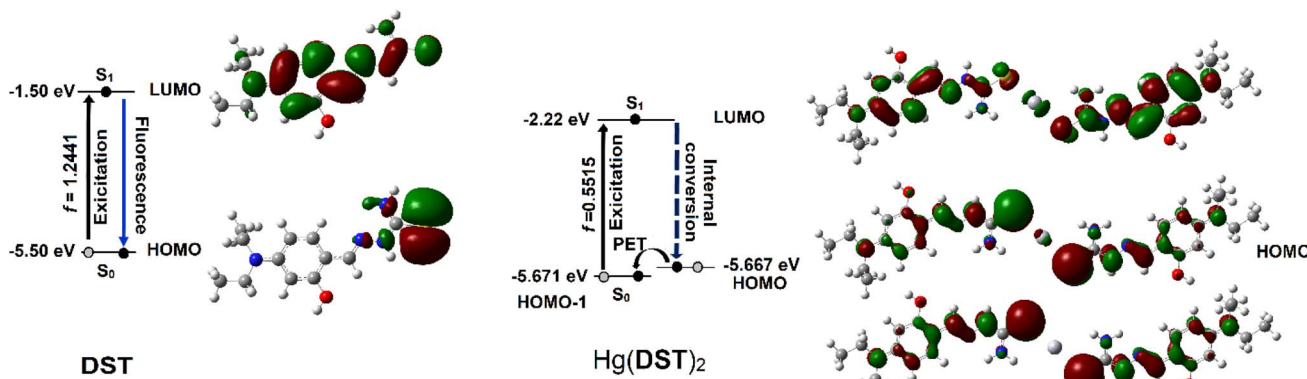


Fig. 4 Diagram illustrating the singlet electron transition processes in the excited state for DST and $\text{Hg}(\text{DST})_2$.

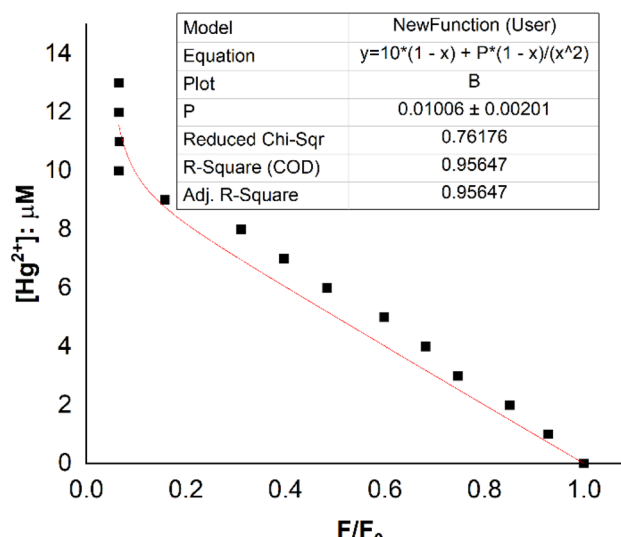


Fig. 5 Nonlinear curve fitting for determining the complexation equilibrium constants of the $\text{Hg}(\text{DST})_2$ complex in an aqueous solution. Where $y = \text{CM}$ represents the total concentration of Hg^{2+} ions added to the solution, with values of 0, 1, 2, 3, 4, 5, 6, 7, 8, 9, 10, 11, 12, and 13 μM . The initial concentration of DST is $C_L = 20 \mu\text{M}$. F_0 and F are the fluorescence intensities of the DST solution when the Hg^{2+} concentration is 0 and C_M , respectively. The reaction occurs in a pH 7.2 phosphate buffer, with an excitation wavelength of 368 nm and an emission wavelength of 445 nm.

normally result in energy emission in the form of fluorescence).^{51–54} Instead, there was an internal conversion process from LUMO to HOMO, resulting in the quenching of fluorescence in the $\text{Hg}(\text{DST})_2$ complex.

3.2. Application of the $\text{Hg}(\text{DST})_2$ sensor for detecting biothiols

3.2.1. Determination of the stability constant of the $\text{Hg}(\text{DST})_2$ complex. To investigate the potential application of the $\text{Hg}(\text{DST})_2$ sensor for detecting biothiols, the experimental stability constant of this complex was first determined using the nonlinear curve-fitting method, based on data obtained from the fluorescence titration of DST with Hg^{2+} .⁵⁵ Here, the complex

formation reaction is represented in eqn (1), and the stability constant of the complex (β_{ex}) is given in eqn (2).



$$\beta_{\text{ex}} = \frac{[\text{Hg}(\text{DST})_2]}{[\text{Hg}^{2+}][\text{DST}]^2} \quad (2)$$

If the initial concentration of DST is denoted as C_L , the initial fluorescence intensity of the DST solution as F_0 , and the fluorescence intensity of the DST solution at equilibrium as F , then let $x = F/F_0$. The concentration of Hg^{2+} used is denoted as $y = \text{CM}$. At equilibrium, the concentrations are expressed as follows:

$$[\text{DST}] = C'_L = C_L \times \frac{F}{F_0} = xC_L \quad (3)$$

$$[\text{Hg}(\text{DST})_2] = C_L \times \frac{(1 - x)}{2} \quad (4)$$

$$[\text{Hg}^{2+}] = y - C_L \times \frac{(1 - x)}{2} \quad (5)$$

Substituting into eqn (2) yields (6) as follows:

$$y = \frac{1}{2}C_L(1 - x) + P\left(\frac{1 - x}{x^2}\right) \quad (6)$$

where:

$$P = \frac{1}{2C_L\beta_{\text{ex}}} \quad (7)$$

when using $C_L = 20 \mu\text{M}$, eqn (6) and (7) become eqn (8) and (9) as follows:

$$y = 10(1 - x) + P\left(\frac{1 - x}{x^2}\right) \quad (8)$$

where:

$$P = \frac{1}{40\beta_{\text{ex}}} \quad (9)$$



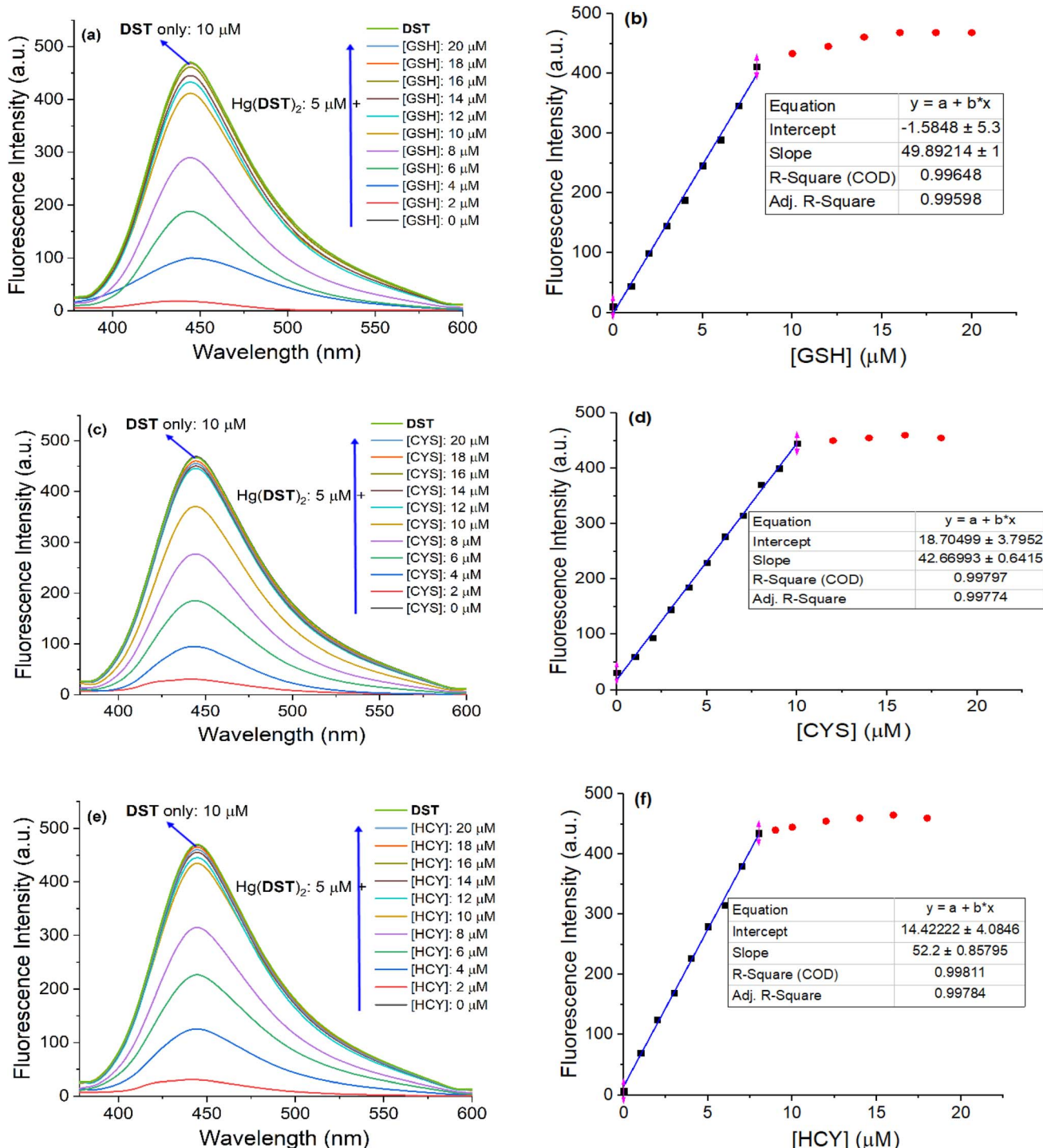


Fig. 6 Fluorescence titration results of the $\text{Hg}(\text{DST})_2$ complex sensor solution (5 μM) by the thiols GSH, Cys, and Hcy (0, 1, 2, 3, 4, 5, 6, 7, 8, 9, 10, 12, 14, 16, 18, 20 μM) in a pH 7.2 phosphate buffer, with an excitation wavelength of 368 nm and an emission wavelength of 445 nm. GSH (a and b), Cys (c and d), and Hcy (e and f).

The fluorescence titration results of the DST solution ($C_L = 20 \mu\text{M}$) with Hg^{2+} (concentrations of 0, 1, 2, 3, 4, 5, 6, 7, 8, 9, 10, 11, 12, and 13 μM) and the nonlinear curve fitted to eqn (8) are presented in Fig. 5. The P value obtained from this process is 0.01006 ± 0.00201 . From eqn (9), the calculated stability constant β_{ex} is $2.458 \mu\text{M}^{-1}$ (or $10^{0.395} \mu\text{M}^{-1}$, equivalent to $10^{12.395} \text{ M}^{-1}$).

3.3. Application of the $\text{Hg}(\text{DST})_2$ sensor for the detection of biothiols

The potential application of the $\text{Hg}(\text{DST})_2$ complex as a fluorescence sensor for detecting GSH, Cys, and Hcy is based on the complex exchange reaction, which depends on the stability constants of the complexes between Hg^{2+} and the ligands GSH,



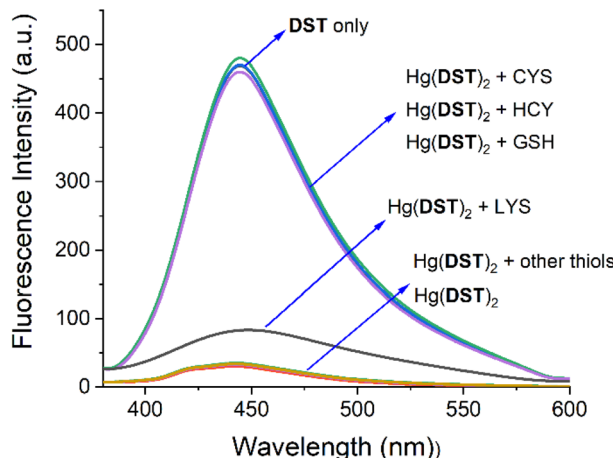


Fig. 7 Fluorescence spectra of the $\text{Hg}(\text{DST})_2$ solution (5 μM) upon addition of thiols GSH, Cys, and Hcy (20 μM each), as well as amino acids Ala, Arg, Asp, Glu, Gly, His, Ile, Leu, Lys, Met, Ser, Thr, Trp, Tyr and Val (20 μM each), in a pH 7.2 phosphate buffer, with an excitation wavelength of 368 nm and an emission wavelength of 445 nm.

Cys, Hcy, and **DST**. For GSH (written as the ligand H_3L), the complexes with Hg^{2+} are detected as ML , MLH , MLH_2 , ML_2 , ML_2H , ML_2H_2 , and ML_2H_3 , with corresponding $\log \beta_{\text{ex}}$ values of 26.04, 32.49, 35.68, 41.58, 42.40, 52.29, and 55.28, respectively.^{56,57} For Cys (written as the ligand $\text{H}_2\text{L}'$), the complexes with Hg^{2+} are detected as ML' , ML'_2 , $\text{ML}'_2\text{H}$ and $\text{ML}'_2\text{H}_2$, with corresponding $\log \beta_{\text{ex}}$ values of 14.21, 43.57, 54.37, and 61.79, respectively.^{56,58-60} For Hcy (written as the ligand $\text{H}_2\text{L}''$), there are still very few published studies on the composition and stability constants of its complexes with Hg^{2+} . One study has identified the existence of the $\text{Hg}\text{L}''_2$ complex, with a stability constant $\log \beta_{\text{ex}}$ determined to be 39.4.⁶¹ In general, previous studies have shown that Hg^{2+} complexes with GSH, Cys, and Hcy exist in various forms, depending on the environment and their concentration ratios. At neutral pH, the predominant species

are ML_2 , ML'_2 , and ML''_2 . Specifically, for GSH, even at a GSH : Hg^{2+} ratio of up to 22 : 1, the ML_2 form still accounts for 95%. For Cys, the proportions of other complexes increase, but ML'_2 remains the dominant species.⁶¹

According to the calculations above, the $\log \beta_{\text{ex}}$ of the $\text{Hg}(\text{DST})_2$ complex is 12.395, much smaller than the $\log \beta_{\text{ex}}$ of the ML_2 , ML'_2 and ML''_2 complexes, which are 41.58, 43.57, and 39.4, respectively. Therefore, theoretically, GSH, Cys, and Hcy can react with $\text{Hg}(\text{DST})_2$ to form corresponding complexes and release free **DST**, altering the fluorescence intensity of the solution. In other words, $\text{Hg}(\text{DST})_2$ can be used as a fluorescence sensor to detect GSH, Cys, and Hcy. One noteworthy point is that since the $\log \beta_{\text{ex}}$ values of the ML_2 , ML'_2 , ML''_2 complexes are approximately similar, it is unlikely that $\text{Hg}(\text{DST})_2$ can selectively detect each thiol in the GSH, Cys, and Hcy group.

Indeed, the experimental results on the fluorescence titration of the $\text{Hg}(\text{DST})_2$ sensor solution by the thiols GSH, Cys, and Hcy, as presented in Fig. 6, are entirely consistent with the aforementioned observations. All three thiols – GSH, Cys, and Hcy – react with $\text{Hg}(\text{DST})_2$, releasing **DST** and leading to an increase in the fluorescence intensity of the solution (The images showing the fluorescence color changes of the $\text{Hg}(\text{DST})_2$ solution in the presence of biothiols, taken inside the fluorescence spectrophotometer chamber, are presented in Fig. S5†). When the concentration of the thiols approaches approximately twice the concentration of $\text{Hg}(\text{DST})_2$ used, as well as beyond this point, the fluorescence intensity of the solution remains nearly unchanged. This indicates that the complexes formed between Hg^{2+} and GSH, Cys, and Hcy are predominantly in the ML_2 , ML'_2 and ML''_2 forms, as previously noted.

The survey results indicate that the $\text{Hg}(\text{DST})_2$ complex sensor can quantitatively detect GSH, Cys, and Hcy, as evidenced by the excellent linear relationship between the fluorescence intensity of the solution and the concentrations of GSH, Cys, and Hcy within a certain range. Accordingly, the linear ranges for determining GSH, Cys, and Hcy using the $\text{Hg}(\text{DST})_2$ sensor are

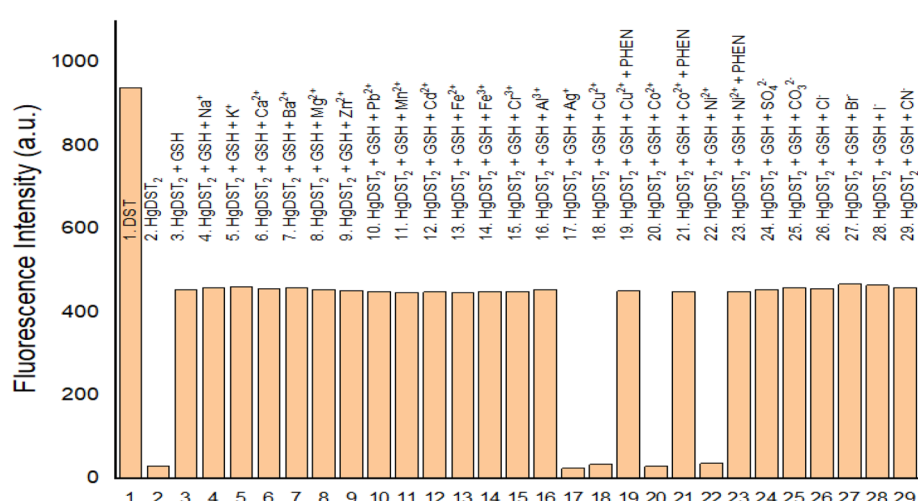
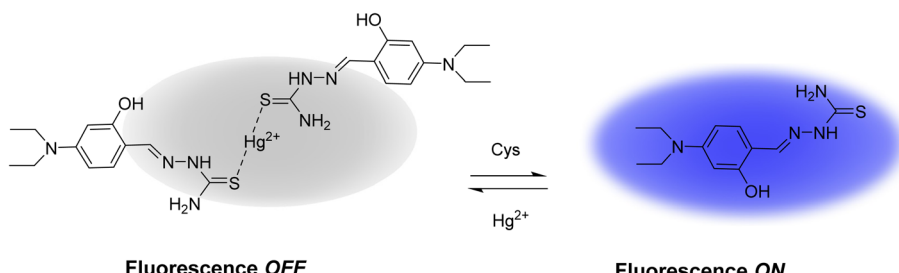


Fig. 8 Fluorescence intensity of solutions: DST (20 μM); $\text{Hg}(\text{DST})_2$ (10 μM); $\text{Hg}(\text{DST})_2$ (10 μM) + GSH (10 μM); $\text{Hg}(\text{DST})_2$ (10 μM) + GSH (10 μM) + metal ions or anions (20 μM); $\text{Hg}(\text{DST})_2$ (10 μM) + GSH (10 μM) + Cu^{2+} , Co^{2+} or Ni^{2+} (20 μM) + PHEN (1500 μM); in a pH 7.2 phosphate buffer, with an excitation wavelength of 368 nm and an emission wavelength of 445 nm.





Scheme 1 Diagram Illustrating the operating principle of the $\text{Hg}(\text{DST})_2$ sensor with biothiols.

0.34–8.00 μM , 0.47–10.00 μM , and 0.26–8.0 μM , respectively, with corresponding linear correlation coefficients (R) of approximately 0.998. Among these, the values of 0.34, 0.47, and 0.26 μM represent the detection limits of GSH, Cys, and Hcy, respectively, using the $\text{Hg}(\text{DST})_2$ sensor, as determined from the calibration curve equation at low concentrations (see Fig. S6 and Table. S1 of the ESI[†]).⁶² Compared to some fluorescent sensors for thiol detection based on metal ion complexes reported in recent times (Table 1), the $\text{Hg}(\text{DST})_2$ sensor had a comparable LOD for thiols but had the advantage of operating in a fully aqueous environment.

The influence of amino acids on the use of the $\text{Hg}(\text{DST})_2$ sensor for thiol detection was also investigated and presented in Fig. 7. The results showed that, except for Lys (lysine), which altered the fluorescence spectrum of the $\text{Hg}(\text{DST})_2$ sensor solution, the other amino acids, including Ala (alanine), Arg (arginine), Asp (aspartic acid), Glu (glutamic acid), Gly (glycine), His (histidine), Ile (isoleucine), Leu (leucine), Met (methionine), Ser (serine), Thr (threonine), Trp (tryptophan), Tyr (tyrosine), and Val (valine), had little to no effect on the fluorescence spectrum of the $\text{Hg}(\text{DST})_2$ sensor solution. These results indicated that the $\text{Hg}(\text{DST})_2$ sensor could detect the thiols GSH, Cys, and Hcy in the presence of the above amino acids, except for Lys. Additionally, the investigation results showed that the $\text{Hg}(\text{DST})_2$ sensor was unable to detect individual thiols within the GSH, Cys, and Hcy groups separately. This finding was consistent with previous reports on fluorescent sensors for thiol detection based on metal ion complexes. However, this limitation did not diminish the applicability of such sensors, as thiols typically do not coexist in equal concentrations in real samples. For instance, in human whole blood samples, GSH is significantly higher than other thiols (sometimes up to 1 mM), whereas, in human plasma samples, Cys is much more abundant than other thiols (sometimes reaching up to 250 μM).^{63–65}

The use of the $\text{Hg}(\text{DST})_2$ complex fluorescent sensor for detecting the thiols GSH, Cys, and Hcy was also investigated for its susceptibility to interference by various ions, including alkali metal ions (Na^+ , K^+), alkaline earth metal ions (Ca^{2+} , Ba^{2+} , Mg^{2+}), transition metal ions (Ag^+ , Cu^{2+} , Co^{2+} , Ni^{2+} , Mn^{2+} , Fe^{2+} , Fe^{3+} , Cr^{3+}), other metal ions (Zn^{2+} , Pb^{2+} , Cd^{2+} , Al^{3+}), as well as common anions such as sulfate (SO_4^{2-}), carbonate (CO_3^{2-}), chloride (Cl^-), bromide (Br^-), iodide (I^-), and cyanide (CN^-). The results, presented in Fig. 8, S7, and S8[†] (in the ESI[†]), demonstrated that, except for Ag^+ , Cu^{2+} , Co^{2+} , and Ni^{2+} , the presence of the other ions did not affect the thiol detection

method using the $\text{Hg}(\text{DST})_2$ sensor, as evidenced by the absence of significant fluorescence intensity changes in $(\text{Hg}(\text{DST})_2 + \text{thiol})$ solutions. The interference caused by Cu^{2+} , Co^{2+} , and Ni^{2+} could be eliminated by the complexing agent 1,10-phenanthroline (PHEN). Meanwhile, a suitable complexing agent to mitigate the interference of Ag^+ has not yet been identified. However, since Ag^+ is not a biological metal, its interference in thiol detection in biological samples is not a major concern.

The reaction time between the $\text{Hg}(\text{DST})_2$ complex and the biothiols GSH, Cys, and Hcy was almost instantaneous. After 1 minute, the fluorescence intensity of the solution had nearly stabilized. The sensing mechanism is summarized in Scheme 1.

4. Conclusions

This study presents the successful development and validation of the $\text{Hg}(\text{DST})_2$ fluorescent sensor for the detection of thiols (GSH, Cys, and Hcy) in aqueous media, achieving detection limits of 0.34, 0.47, and 0.26 μM , respectively. The sensor exhibited robust selectivity against most common amino acids, metal ions, and anions, with interference from Cu^{2+} , Co^{2+} , and Ni^{2+} effectively neutralized using 1,10-phenanthroline (PHEN), while Ag^+ interference remains negligible in biological contexts due to its non-physiological relevance. Compared to existing metal-complex-based fluorescent sensors, $\text{Hg}(\text{DST})_2$ offers comparable sensitivity and the distinct advantage of operating in a fully aqueous environment. These attributes position $\text{Hg}(\text{DST})_2$ as a highly effective and practical tool for real-time thiol monitoring in biomedical diagnostics (e.g., oxidative stress assessment) and environmental analysis.

Data availability

The data supporting this article have been included as part of the ESI.[†]

Conflicts of interest

There are no conflicts to declare.

Acknowledgements

This research was funded by the Vietnam National Foundation for Science and Technology Development (NAFOSTED) under grant number 104.06-2021.59 (Nguyen Khoa Hien).



References

- 1 G. Chwatko and E. Bald, *Talanta*, 2000, **52**, 509–515.
- 2 C. X. Yin, K. M. Xiong, F. J. Huo, J. C. Salamanca and R. M. Strongin, *Angew. Chem., Int. Ed.*, 2017, **56**, 13188–13198.
- 3 D. Chen and Y. Feng, *Crit. Rev. Anal. Chem.*, 2022, **52**, 649–666.
- 4 S. M. Nabavi and A. S. Silva, *Nonvitamin and Nonmineral Nutritional Supplements*, Academic Press, 2018.
- 5 Y. Yue, F. Huo, P. Ning, Y. Zhang, J. Chao, X. Meng and C. Yin, *J. Am. Chem. Soc.*, 2017, **139**, 3181–3185.
- 6 D. Matuz-Mares, H. Riveros-Rosas, M. M. Vilchis-Landeros and H. Vázquez-Meza, *Antioxidants*, 2021, **10**, 1220.
- 7 R. Vona, L. Pallotta, M. Cappelletti, C. Severi and P. Matarrese, *Antioxidants*, 2021, **10**, 201.
- 8 J. Pizzorno, *Integr. Med.*, 2014, **13**, 8.
- 9 J. Selhub, *Annu. Rev. Nutr.*, 1999, **19**, 217–246.
- 10 Y. Li, L. Chen, Y. Zhu, L. Chen, X. Yu, J. Li and D. Chen, *RSC Adv.*, 2021, **11**, 21116–21126.
- 11 I. M. Graham, L. E. Daly, H. M. Refsum, K. Robinson, L. E. Brattström, P. M. Ueland, R. J. Palma-Reis, G. H. Boers, R. G. Sheahan and B. Israelsson, *JAMA*, 1997, **277**, 1775–1781.
- 12 D. S. Wald, M. Law and J. K. Morris, *BMJ*, 2002, **325**, 1202.
- 13 K. S. McCully, *Am. J. Pathol.*, 1969, **56**, 111.
- 14 A. D. Smith, S. M. Smith, C. A. De Jager, P. Whitbread, C. Johnston, G. Agacinski, A. Oulhaj, K. M. Bradley, R. Jacoby and H. Refsum, *PLoS One*, 2010, **5**, e12244.
- 15 M. Isokawa, T. Funatsu and M. Tsunoda, *Analyst*, 2013, **138**, 3802–3808.
- 16 C.-J. Tsai, F.-Y. Liao, J.-R. Weng and C.-H. Feng, *J. Chromatogr. A*, 2017, **1524**, 29–36.
- 17 I. M. Mostafa, H. Liu, S. Hanif, M. R. H. S. Gilani, Y. Guan and G. Xu, *Anal. Chem.*, 2022, **94**, 6853–6859.
- 18 P. Li, S. M. Lee, H. Y. Kim, S. Kim, S. Park, K. S. Park and H. G. Park, *Sci. Rep.*, 2021, **11**, 3937.
- 19 N. K. Hien, M. Van Bay, P. D. Tran, N. T. Khanh, N. D. Luyen, Q. V. Vo, D. U. Van, P. C. Nam and D. T. Quang, *RSC Adv.*, 2020, **10**, 36265–36274.
- 20 D. T. Nhan, N. K. Hien, H. Van Duc, N. T. A. Nhung, N. T. Trung, D. U. Van, W. S. Shin, J. S. Kim and D. T. Quang, *Dyes Pigments*, 2016, **131**, 301–306.
- 21 H. J. Park, C. W. Song, S. Sarkar, Y. W. Jun, Y. J. Reo, M. Dai and K. H. Ahn, *Chem. Commun.*, 2020, **56**, 7025–7028.
- 22 L. Chen, Y. Feng, Y. Dang, C. Zhong and D. Chen, *Anal. Bioanal. Chem.*, 2020, **412**, 7819–7826.
- 23 D. Chen, Z. Long, Y. Sun, Z. Luo and X. Lou, *J. Photochem. Photobiol. A*, 2019, **368**, 90–96.
- 24 K. Dou, W. Huang, Y. Xiang, S. Li and Z. Liu, *Anal. Chem.*, 2020, **92**, 4177–4181.
- 25 L. Chen, L. Sun, L. Ye and Y. Wang, *Opt. Mater.*, 2020, **106**, 109961.
- 26 L. Flohé, *Glutathione*, CRC Press, 2018.
- 27 L. Yuan and N. Kaplowitz, *Mol. Aspects Med.*, 2009, **30**, 29–41.
- 28 P. Ganguly and S. F. Alam, *Nutr. J.*, 2015, **14**, 1–10.
- 29 L. Zhou, J. Liu, Y. An, Y. Wang and G. Wang, *Front. Cardiovasc. Med.*, 2022, **9**, 898305.
- 30 B. Sameem, F. Khan and K. Niaz, in *Nonvitamin and Nonmineral Nutritional Supplements*, Elsevier, 2019, pp. 53–58.
- 31 M. Vairetti, L. G. Di Pasqua, M. Cagna, P. Richelmi, A. Ferrigno and C. Berardo, *Antioxidants*, 2021, **10**, 364.
- 32 Y. Hu, C. H. Heo, G. Kim, E. J. Jun, J. Yin, H. M. Kim and J. Yoon, *Anal. Chem.*, 2015, **87**, 3308–3313.
- 33 H. Jia, M. Yang, Q. Meng, G. He, Y. Wang, Z. Hu, R. Zhang and Z. Zhang, *Sensors*, 2016, **16**, 79.
- 34 Q. Li, Y. Guo and S. Shao, *Sens. Actuators, B*, 2012, **171**, 872–877.
- 35 S. Li, D. Cao, X. Meng, Z. Hu, Z. Li, C. Yuan, T. Zhou, X. Han and W. Ma, *Bioorg. Chem.*, 2020, **100**, 103923.
- 36 Y. Wang, H. Feng, H. Li, X. Yang, H. Jia, W. Kang, Q. Meng, Z. Zhang and R. Zhang, *Sensors*, 2020, **20**, 1331.
- 37 Y. Wang, Q. Meng, Q. Han, G. He, Y. Hu, H. Feng, H. Jia, R. Zhang and Z. Zhang, *New J. Chem.*, 2018, **42**, 15839–15846.
- 38 N. Kaur, P. Kaur and K. Singh, *RSC Adv.*, 2014, **4**, 29340–29343.
- 39 C. Zhao, X. Kong, S. Shuang, Y. Wang and C. Dong, *Analyst*, 2020, **145**, 3029–3037.
- 40 Y. Hu, L. Lu, S. Guo, X. Wu, J. Zhang, C. Zhou, H. Fu and Y. She, *Sens. Actuators, B*, 2023, **382**, 133534.
- 41 M. J. Frisch, G. W. Trucks, H. B. Schlegel, G. E. Scuseria, M. A. Robb, J. R. Cheeseman, G. Scalmani, V. Barone, G. A. Petersson, H. Nakatsuji, X. Li, M. Caricato, A. V. Marenich, J. Bloino, B. G. Janesko, R. Gomperts, B. Mennucci, H. P. Hratchian, J. V. Ortiz, A. F. Izmaylov, J. L. Sonnenberg, D. Williams-Young, F. Ding, F. Lipparini, F. Egidi, J. Goings, B. Peng, A. Petrone, T. Henderson, D. Ranasinghe, V. G. Zakrzewski, J. Gao, N. Rega, G. Zheng, W. Liang, M. Hada, M. Ehara, K. Toyota, R. Fukuda, J. Hasegawa, M. Ishida, T. Nakajima, Y. Honda, O. Kitao, H. Nakai, T. Vreven, K. Throssell, J. A. Montgomery Jr, J. E. Peralta, F. Ogliaro, M. J. Bearpark, J. J. Heyd, E. N. Brothers, K. N. Kudin, V. N. Staroverov, T. A. Keith, R. Kobayashi, J. Normand, K. Raghavachari, A. P. Rendell, J. C. Burant, S. S. Iyengar, J. Tomasi, M. Cossi, J. M. Millam, M. Klene, C. Adamo, R. Cammi, J. W. Ochterski, R. L. Martin, K. Morokuma, O. Farkas, J. B. Foresman and D. J. Fox, *Gaussian 16 Revision A. 03. 2016*, Gaussian inc, Wallingford CT, 2016.
- 42 C. Adamo and V. Barone, *J. Chem. Phys.*, 1999, **110**, 6158–6170.
- 43 A. D. Laurent and D. Jacquemin, *Int. J. Quantum Chem.*, 2013, **113**, 2019–2039.
- 44 C. Lee, W. Yang and R. G. Parr, *Phys. Rev. B: Condens. Matter Mater. Phys.*, 1988, **37**, 785.
- 45 D. Jacquemin, I. Duchemin and X. Blase, *J. Chem. Theory Comput.*, 2015, **11**, 5340–5359.
- 46 C. Adamo and D. Jacquemin, *Chem. Soc. Rev.*, 2013, **42**, 845–856.
- 47 J. Tomasi, B. Mennucci and R. Cammi, *Chem. Rev.*, 2005, **105**, 2999–3094.



48 N. K. Hien, M. Van Bay, Q. V. Vo, D. T. Quang and P. C. Nam, *J. Fluids*, 2024, 1–13.

49 K.-W. Ding, T.-Q. Li, Z.-X. Ge, J.-H. Bu and Y. Liu, *RSC Adv.*, 2018, **8**, 35759–35767.

50 K. Fenner, G. Reynolds and S. Basu, *Spectrochim. Acta, Part A*, 2020, **239**, 118473.

51 N. K. Hien, N. C. Bao, N. T. A. Nhun, N. T. Trung, P. C. Nam, T. Duong, J. S. Kim and D. T. Quang, *Dyes Pigments*, 2015, **116**, 89–96.

52 M. V. Bay, N. K. Hien, S. Son, N. D. Trinh, N. T. Trung, P. C. Nam, J. S. Kim and D. T. Quang, *Sensors*, 2019, **19**, 128.

53 N. K. Hien, D. T. Nhan, W. Y. Kim, M. Van Bay, P. C. Nam, D. U. Van, I.-T. Lim, J. S. Kim and D. T. Quang, *Dyes Pigments*, 2018, **152**, 118–126.

54 D. T. Nhan, N. T. A. Nhun, V. Vien, N. T. Trung, N. D. Cuong, N. C. Bao, D. Q. Huong, N. K. Hien and D. T. Quang, *Chem. Lett.*, 2017, **46**, 135–138.

55 J.-S. Wu, F. Wang, W.-M. Liu, P.-F. Wang, S.-K. Wu, X. Wu and X.-H. Zhang, *Sens. Actuators, B*, 2007, **125**, 447–452.

56 W. Stricks and I. Kolthoff, *J. Am. Chem. Soc.*, 1953, **75**, 5673–5681.

57 P. D. Oram, X. Fang, Q. Fernando, P. Letkeman and D. Letkeman, *Chem. Res. Toxicol.*, 1996, **9**, 709–712.

58 G. Lenz and A. Martell, *Biochemistry*, 1964, **3**, 745–750.

59 D. Perkins, *Biochem. J.*, 1953, **55**, 649.

60 K. Dubey and M. Qazi, *Proc. Natl. Acad. Sci., India*, 1983, **53**, 342–346.

61 V. Liem-Nguyen, U. Skyllberg, K. Nam and E. Björn, *Environ. Chem.*, 2017, **14**, 243–253.

62 Y. Liu, T. B. Ren, D. Cheng, J. Hou, D. Su and L. Yuan, *ChemistryOpen*, 2019, **8**, 1251–1257.

63 X. Fu, S. A. Cate, M. Dominguez, W. Osborn, T. Özpolat, B. A. Konkle, J. Chen and J. A. López, *Sci. Rep.*, 2019, **9**, 115.

64 P. Hallman, D. Perrin and A. E. Watt, *Biochem. J.*, 1971, **121**, 549–555.

65 P. M. Ueland, H. Refsum, S. P. Stabler, M. R. Malinow, A. Andersson and R. H. Allen, *Clin. Chem.*, 1993, **39**, 1764–1779.

